Physico-mechanical properties of nano polystyrene decorated graphene oxide-epoxy composites.

KHOBRAGADE, P.S., HANSORA, D.P., NAIK, J.B., NJUGUNA, J. and MISHRA, S.

2017

Physico-mechanical properties of nano polystyrene (nPS) decorated graphene oxide (GO) -epoxy composites

Prashant S. Khobragade[1], D.P. Hansora[1], Jitendra B. Naik[1], James Njuguna[2], Satyendra Mishra[1]*

[1]*University Institute of Chemical Technology, North Maharashtra University, Jalgaon-425001, Maharashtra, India*

[2]*School of Engineering, Robert Gordon University, Riverside East, Aberdeen, AB10 7GJ, United Kingdom*

Corresponding address: Email: *profsm@rediffmail.com

Tel.: +91-257-2258420. Fax: +91-257-2258403.

Abstract

In this work, nano polystyrene (nPS) decorated graphene oxide (GO) hybrid nanostructures were successfully synthesized using stepwise micro emulsion polymerization, and characterized by Fourier transform infrared spectroscopy (FTIR), X-ray diffractometer (XRD), field-emission scanning electron microscopy (FE-SEM) and transmission electron microscopy (TEM). XRD and FTIR spectra revealed the existence of a strong interaction between the nPS and GO, which implies that the polymer chains were successfully grafted onto the surface of the GO. The nPS decorated GO hybrid nanostructures were compounded with epoxy by hand lay-up technique, and the effect of the nPS-GO on the mechanical, thermal and surface morphological properties of the epoxy matrix was investigated by Universal tensile machine (UTM), Izod impact tester, thermogravimetric analysis (TGA) and contact angle measurement by a goniometer. It was observed that in the epoxy matrix, GO improved the compatibility.

1. Introduction

Epoxy resins are an important class of thermosetting polymers widely used in the applications of printing circuit board, insulator, adhesive, insulation, various electrical tools, coatings, structural components and matrices for fibrous composites for their engineering structural applications [1, 2]. Among the various polymer matrices available, epoxy resins remain dominant in the development of high performance materials due to their thermal stability, mechanical properties, process ability, excellent electrical insulation, low shrinkage, excellent combination of stiffness, satisfactory adhesion, solvent resistance strength, chemical resistance, insulating properties and environmental stability. Some of the disadvantages of cross linked epoxy limit their structural engineering applications [3-4]. The main drawback of epoxy resins for structural applications maybe its inherent brittleness. Several research and scientific investigations have been devoted to the reinforcement of epoxy matrices with various nanostructured materials; so numerous attempts have been carried out to improve their performance, especially the fracture toughness.[5-7] Fiber reinforcement into toughen epoxy matrix is widely used as a common way to improve the toughness and other properties of the composites.[8] But developing the advanced multifunctional polymer composites represents a class of functional materials with multifunctional tailored properties that include enhanced thermal and mechanical stability, and they can be developed for lightweight applications such as aerospace structural components, jet engine parts, actuators, adaptive smart materials, and robust durable materials using multifunctional polymer nanocomposites.[9-10] In recent years, researchers have focused on the modifying and improvising the properties of epoxies using different fillers, including graphene and modified graphene.[11-14] Graphene oxide (GO) has a tremendous interest in a scientific research, because GO is a two dimensional (2D) and conducting layered material; it consists of one atom-thick planar sheets of sp2-bonded honeycomb structure of carbon atoms. GO possesses extraordinary mechanical, thermal, electronic and physical

properties, more importantly, it contains a range of reactive oxygen functional groups (e.g., hydroxyl and epoxy groups). Therefore, graphene is a basic building block of graphitic materials having all dimensionalities and used in the synthesis of varieties of composite blend films and polymer nanocomposites. However, graphene sheets have a high specific surface area, which tend to form irreversible agglomerates or even restack to form graphite through Van der Waals interactions.[15-25] So, many scientists prepared hybrid nanostructures of GO with different organic and inorganic materials to overcome this problem of GO. Organic/inorganic hybrid materials can now be fully integrated in the field of nanosciences. They are multifunctional by nature, and it can be used as innovative advanced materials. They can also act as precursors to new materials with highly attractive properties. Recently, different researchers reported the modification of graphene with different organic/inorganic materials such as phosphorus-nitrogen containing dendrimer[26], polyvinylidene fluoride [27], styrene treated maleic anhydride[28], silica[29], carbon nanotubes[30] and metal nanoparticle[31] to improve the dielectric, rheological, electrical, sensing and conducting properties respectively of the polymers.

In this research work, we have confirmed nPS decorated GO strengthened into the epoxy matrix with extended mechanical, thermal as well as physical properties. We further showed that the much less wt. % (0 to 0.7 wt. %) of nPS decorated GO hybrid nanostructures possessed the mechanical, thermal and physical properties, due to exfoliation and interfacial interplay. In this work, a facile and strong approach are mentioned for improving the dispersion of GO through hybridization.

2. Experimental section

2.1. Materials

Hand Lay-up Epoxy matrix and hardener, grade name Lapox L-12 and K-6 were procured from polymer division of Atul Limited, Mumbai, India. GO sheets, with average 50 nm in thickness and up to the certain μm in length were synthesized by modifying Hummers method[15]. Styrene (St) as monomer; ammonium persulfate (APS) as the initiator; sodium dodecyl sulfate (SDS) as surfactants, were procured from Sigma Aldrich, Mumbai, India. St was treated with 5% NaOH aqueous solution to remove the inhibitor. All other materials were of analytical grade, and used without further purification. Deionised (DI) water was used throughout the experiment. Solvents like acetone, ethanol and toluene for washing purpose were procured from Sigma Aldrich, Mumbai, India.

2.2. Synthesis of nPS decorated graphene oxide

nPS decorated GO hybrid nanostructures were easily prepared by stepwise micro emulsion polymerization[32]. In general, hybrid nanostructures were synthesized using a two-step process. In this synthesis technique the first GO were synthesized by modified Hummers method and separately incorporated into oil/water (o/w) micro emulsion system with prior sonication. The St was added dropwise into the microemulsion system for coating the nPS material onto the surface of GO. The typical recipes were used as per follows: About 250 mg GO was dispersed in 100 mL DI water taken in a 250 mL round-bottom flask. 0.1 g SDS was added into the flask, followed by 15 min of ultrasonic irradiation. Afterwards, 0.1 g APS was added into the mixture and the reaction mixture was allowed to stirr, followed by dropwise addition of 10g St monomer into the reaction system was continued for another 1.5 h at 75±5 °C and stopped by cooling the dispersion to room temperature. A translucent dispersion was formed after the complete polymerization reaction, which indicated the formation of microemulsion filtered through a PTFE membrane, and then

washed with DI water and acetone to remove impurities. The purified product was dried in vacuum oven, at 60 °C, resulting in a gray-black solid.

2.3 Preparation of nPS decorated GO filled epoxy nanocomposites

For the preparation of 0.1, 0.2, 0.3, 0.4, 0.5, 0.6, and 0.7 wt. % nanocomposites, hand Lay-up Epoxy matrix and hardener, grade name Lapox L-12 and K-6 was procured from polymer division of Atul Limited, Mumbai, India was used as the polymer matrix. The nPS decorated GO/acetone suspension was added to the resin and stirred simultaneously with heating up to 60 °C for 12 h for slow solvent evaporation. An additional 12 h of heating under vacuum conditions ensured the complete acetone removal. The hardener was added to the dispersions at a weight ratio of 100:6 and mixed for 5 min. The resulting mixtures were poured into a Teflon mold. In order to characterize and testing, the dumbbell and strip samples were cut from the sheets [33, 34].

2.4. Characterization

Functional groups of Graphite, GO, nPS and nPS decorated GO were recorded on FTIR spectrophotometer (FTIR-8000 Spectrophotometer, Shimadzu, Tokyo, Japan). The number of scans per sample was 25 and resolutions of the measurements were 4 cm^{-1}. The recorded wave number range was 500-4000 cm^{-1}. For the structural analysis synthesized graphite,GO, nPS and nPS decorated GO were characterized by using X-ray diffractometer (XRD, Bruker D8 Advance, Berlin, Germany) in the range of 5-80º. The samples were placed vertically in front of the X-ray source. The detector was moving at an angle of 2θ while the sample was moving at an angle of θ at the wavelength $\lambda = 1.54$ Å (Cu Kα, a tube voltage 40 kV and tube current 25 mA). Topographical surface morphology of GO, nPS, nPS decorated GO were determined by using field emission scanning electron microscope (FE-SEM, S-4800 Hitachi, Tokyo, Japan) operated at an

accelerating voltage of 30 kV) and backscattered electron techniques as transmission electron microscope (TEM, Philips CM-200, Eindhoven, The Netherlands) with 75 µA of filament current and 200 kV of accelerating voltage. The mechanical properties like tensile strength (TS), elongation at break (EB) and young's modulus were measured as per ASTM-D 412 using UTM (2302 R & D Equipment, Mumbai). Crosshead speed was 50 mm/min and impact strength was measured on the izod impact tester (International equipments, Mumbai). Thermal stability and degradation properties of the GO, nPS decorated GO and nPS decorated GO filled epoxy nanocomposites were determined by a thermo gravimetric analyzer (TGA-50, Shimadzu, Tokyo, Japan). 10 mg of sample was placed in a Pt pan for TGA measurement. The temperature was programmed from 30 to 600 °C at a heating rate of 10 °C/min under a nitrogen atmosphere to avoid thermoxidative degradation. All samples were run two times. Contact angle measurements of pristine epoxy and nPS decorated GO filled epoxy nanocomposites were carried out by the sessile drop method using DI water as a probe liquid on contact angle goniometer (Model-200 P/N 200-FU, Rame Hart, USA). All samples were kept in powdered solid form and analyzed at room temperature.

3. Results and discussion

3.1. Surface functionalization of nPS decorated GO nanostrucutres

The FT-IR spectra of Graphite, GO, nPS and nPs decorated GO composites are shown in Fig. 1 (a-d). The GO shows strong and broad peak at 3360 cm^{-1} seen in Fig. 1 (b) indicates the presence of surface O–H stretching due to the vibrations of the H-O-H groups of water. The other peaks correspond to oxygen functional groups, such as carboxyl (C=O) stretching of COOH groups (1725 cm^{-1}), aromatic (C=C) stretching (1615 cm^{-1}), epoxy (C–O) group stretching (1218 cm^{-1}) and alkoxy (C–OH) group stretching vibrations (1043 cm^{-1})[15]. In the FTIR spectra of nPS, the

absorption bands at 3027, 2885, 1491, 1369 and 756 cm^{-1}, respectively revealed the stretching of the C-H bond in the phenyl ring, the asymmetric stretching of the C-H bond, symmetric stretching of C-H bond and rocking of C-H bond in the aromatic phenyl ring of nPS, while the peaks at 905 and 840 cm^{-1} are attributed to the amorphous portions of the nPS (Fig. 1 (c)) [35]. Fig. 1 (d), shows the corresponding peaks to same oxygen functional groups, such as carboxyl (C=O) stretching of COOH groups (1725 cm^{-1}), aromatics (C=C) stretching (1615 cm^{-1}), epoxy (C–O) group stretching (1218 cm^{-1}) and alkoxy (C–OH) group stretching vibrations (1043 cm^{-1}) and the same absorption bands at 3027, 2885, 1491, 1369, and 756 cm^{-1} respectively. This revealed the stretching of the C-H bond in the phenyl ring of nPS[36]. The presence of both carboxyl groups and stretching of phenyl ring of PS in the spectra of nPS decorated GO confirmed the formation of hybrid nanostructures.

3.2. Structural, crystallinity and morphological analyses of nPS decorated GO nanostrucutures

The crystal structure as well as the orientation of nPS decorated GO were studied from XRD analysis, which also verified the average spacing between Graphite, GO, nPS and nPS decorated GO. Fig. 2 (a) shows the XRD patterns of pristine graphite. A sharp and high-intensity peak at 2θ = 26.58° was detected, which corresponded to the well-arranged layer structure with d-spacing of 0.335 nm along the (002) orientation. In addition, a small Bragg reflection of graphite phase (004) was also detected at 2θ value of 54.73° with d-spacing of 0.17 nm[37]. The diffraction peak of exfoliated GO was recorded at 2θ = 10.11°, which attributes to the plane of GO (0 0 2) features 0.71 Fig. 2 (b). This also shows the complete oxidation of graphite into the GO due to the introduction of oxygen-containing functional groups on the graphene sheets. On the other hand, the XRD pattern of nPS exhibits the broad, amorphous peak centered at 2θ = 19.5° and no other peaks were observed (Fig. 2(c)). This signifies that a purely amorphous region is present in the

nPS. To further confirm the structures, the powder XRD patterns (Fig. 2 (d)) of nPS decorated GO were recorded; the diffraction peak (0 0 2) was appeared at around $2\theta=9.2$ and the interlayer space was about 0.35 nm. For the nPS decorated GO, the diffraction peak (0 0 2) plane was shifted to lower diffraction angle resulting an increase in d spacing between GO sheets due to the attachment of nPS microspheres along the edges of the stacked nanosheets, which disrupts the van der Waals interactions and enlarges the-spacing of the nanosheets [32].

Typical FE-SEM and TEM images of GO, nPS and nPS decorated GO are shown in Figs. 3 and 4. GO exhibited the exfoliated layered structure with scrolled multilayer sheets with thin, transparent, smooth, wrinkled and folded on the basal and edges with an average 50 nm in thickness and up to the certain μm in length (Fig. 3a and 4a). The surface morphology of the nPS is also presented in Fig. 3b and 4b. Their morphology was observed circular in shape and the particle surface was observed to be smooth with an average diameter of 80 nm.

The surface morphology of the hybrid nPS decorated GO was also studied and shown in Fig. 3c and 4c. The corresponding images show significant morphological differences with respect to the GO, it can be assured that nPS get attached uniformly on the edges of GO sheets and considerately amplifies the distances between adjacent GO sheets. Scheme 1 shows the reaction mechanism of nPS with GO, a nucleophilic attack of styrene on oxyrane for ring opening to form O⁻ and carbocation intermediate in one compound. FTIR, XRD, morphological results and a schematic representation of nPS decorated GO also confirm the formation of hybrid nanostructures.[35, 38, 39]

3.3. Mechanical properties of nPS decorated GO filled epoxy nano composites

Tensile strength (TS) and elongation at break (EB), Youngs modulus and impact test of epoxy nano composites at various wt. % loadings of nPS decorated GO are shown in Fig. 5. The highest

(32 MPa) TS of nanocomposites was observed at 0.3 wt. % loading. This was due to the greater intermolecular reinforcing interaction and exfoliations between nPS decorated GO in epoxy matrix (Fig.5 (a)). However, the TS were observed in decreasing trend for 0.1, 0.2 and from 0.4 wt. % loadings due to less interfacial interaction at very low loading and filler aggregation at higher loading. This indicated that better interaction and exfoliation of nPS decorated GO was improved at lower (0.3 wt. %) loading. It is also evident from Fig. 5 (b) that the EB of epoxy nanocomposites increased up to 0.2 wt. % loading and decreased for 0.3 wt. % loading and again increased for 0.4 to 0.7 wt. % loadings of nPS decorated GO. At the early stage (0.3 wt. %), EB was very low due to the perfect amount of exfoliated nanomaterials which were restricting the polymer chains for intermolecular movement, the enhancement of elongation was the high resistance exerted by well exfoliated nanostructures against the chain deformation and the stretching resistance. The Young's modulus (Fig. 5 (c)) defined the stress required breaking a sample; it also strongly depended on the tensile strength. The average data of Young's modulus of the composite samples with the same nPS decorated content with a small loading (0.3 wt. %) show significant improvement in the Young's modulus. For epoxy nanocomposites, the TS was reported to be 32 MPa at 0.3 wt. % and the Young's modulus was reported to be 424 MPa. The impact strength (Fig.5 (d)) of the epoxy nanocomposites with different wt. % loading was also reported. It can be seen that the suitable amount of fillers can properly improve the impact strength of epoxy resin. Unfortunately, the impact strength of the composites declined when the amount of fillers was further increased, which is due to the fact that excessive fillers cannot be well dispersed in the matrix and agglomerate to cluster.[40-46] The values of the mechanical properties also mention in the Table 1.

3.4. *Thermal behavior of nPS decorated GO filled epoxy nanocomposites*

The TGA of the GO, nPS, nPS decorated GO and epoxy nanocomposites are shown in Fig. 6. The pristine GO exhibited single step degradation with significant mass loss at around 180 °C due to

the pyrolysis of the labile oxygen-containing functional groups. The presence of the oxygen functional groups makes GO thermally unstable, as it undergoes pyrolysis at elevated temperatures (Fig. 6a). Mass loss was recorded up to 90% below 200 °C mainly due to the decomposition of oxygen-containing groups and the loss of interlayer water molecules. [16, 47] The nPS showed the thermal decomposition pattern with 100 % mass loss at d_{on} = 372 °C (Fig. 6b).[31] A remarkable difference is observed in the thermal behavior of the nPS decorated GO. The nPS decorated GO (Fig. 6 (c)) shows a high thermal stability (d_{on}= 424 °C) and (d_{off}= 460 °C) with a 100 % weight loss. This different behavior further demonstrated the existence of a strong interaction between the nPS and the GO sheets. Fig. 7 shows the TGA curves of pure epoxy and its composites containing different loadings of nPS decorated GO. Fig. 7, all the samples begin to decompose at 370-380 °C and degrade almost completely below 440 °C due to the pyrolysis of polymer main-chains. It should be noted that the thermal stabilization d_{on} of the composites was observed to be increased with increase in nPS decorated GO loading (Fig. 7 and Table 1). The higher d_{on} degradation temperatures were recorded to be 376 °C and 379 °C for the 0.5 and 0.6 wt. % loadings and d_{off} temperature recorded as 438 °C (Table 1). The presence of nPS decorated GO sheets in the composites inhibits the mobility of epoxy chains and increases its onset degradation temperature; the reason behind it is "tortuous path" effect to delay the escape of volatile degradation products and the permeation of oxygen and char formation, which is likely responsible for the improvement in d_{on} temperature. And for d_{off}, the 0.1 wt.% loading shows better d_{off} properties because of at lower loading the hybrid nanostructures were well exfoliated and no char formation was occurred at early temperature.[48-51]

3.5. Surface contact angle of nPS decorated GO filled epoxy nanocomposites

The surface wettability of the nanocomposites was examined by water contact angle (WCA) measurements, where the contact angle depends upon the hydrophobic or the hydrophilic character of the surface. A contact angle characterization permits the actual physical properties of the surface; thus one can fully describe the surface morphology of the nanocomposites system. The contact angle micrographs of the neat epoxy and its 0.3, 0.5 and 0.7 wt. % loading composites are shown in Fig. 8. The hybrid nanocomposites with low contents up to 0.3 wt. %. loading show better good hydrophobic properties with a DI water contact angle of 62° (Fig. 8 (b)) as compared to epoxy, 0.5 (60°) and 0.7 (58°) wt. % (Fig.8 (c and d). It is expected that the excellent exfoliation of nanostructures contributes to significant improvement in physical properties of epoxy hybrid nanocomposites. As expected, the hydrophobicity of the 0.3 wt. % is higher than that of other composites owing to the high level of grafting, the dispersibility and stability of the hybrid nanostructures. The reduced contact angle of the nanocomposites is owing to the relative absence of ungrafted nPS decorated GO present in the epoxy matrices.

4. Conclusion

Hybrid nanostrucutres of nPS decorated GO were successfully synthesized by a step wise microemulsion polymerization technique. The obtained nPS decorated GO possessed a perfect hybrid structures, which was formed via bonding of nPS to the GO nano sheets. The XRD patterns and FTIR spectra confirmed the interaction of nPS and GO, while the increased thermal stability also suggested that a definite interaction occurred during polymerization. A small amount of nPS decorated GO nanostructures (0 - 0.7 wt. %) was introduced to improve the thermal, mechanical and surface morphology, properties of epoxy hybrid nanocomposites. It revealed that these hybrid nanostructures exhibited a synergistic effect on thermal, mechanical and physical properties. After adding hybrid nanostructures, epoxy hybrid nanocomposites showed significant variation when a

lower amount of hybrid nanostructures (up to the 0.7 wt. % loading) was incorporated in an epoxy matrix.

References

1 Yoonessi M, Lebron-Colon M, Scheiman D, Meador M A, *ACS Appl Mater Interfaces* **19**:16621−16630 (2014).

2 Wang W, Pan H, Shi Y, Pan Y, Yang W, Liew K M, Song L, Hu Y, *Composites Part A Appl Sci and Manu* **80**:259–269 (2016).

3 Wang F, Drzal L T, Qin Y and Huang Z, *Composites Part A Appl Sci and Manu* **87**:10-22(2016).

4 Shen X J, Liu Y, Xiao H M, Feng Q P, Yu Z Z, Fu S Y, *Compo Sci and Tech* **72**:1581–1587(2012).

5 Wan Y J, Gong L X, Tang L C, Wu L B, Jiang J X, *Composites Part A Appl Sci and Manu* doi.org/10.1016/j.compositesa.2014.04.023.

6 Li D, Liu Y, Sui G, *Composites Part A Appl Sci and Manu* **84**:87–95 (2016).

7 Pour Z S, Ghaemy M, *Compo Sci and Tech* **136**:145-157 (2016).

8 Carvelli V, Betti A, Fujii T, *Composites Part A Appl Sci and Manu* **84**: 26–35(2016).

9 Mortazavi B, Benzerara O, Meyer H, Bardon J, Ahzi S, *Carbon* **60**:356-365 (2013).

10 Thitsartarn W, Xiaoshan F, Yang S, Chuan J Y C, Du Y, Chaobin H, *Compo Sci and Tech* **118**:63-71(2015).

11 Chatterjee S, Nafezarefi F, Tai N H, Schlagenhauf L, Nuesch F A, Chu B T T, *Carbon* **50**: 5380 –5386 (2012).

12 Zabihi O, Ahmadi M, Shafei S, Seraji S M, Oroumei A, Naebe M, *Composites Part A App Sci and Manu* **88**: 243–2522(2016).

13 Garlof S, Fukuda T, Mecklenburg M, Smazna D, Mishra Y K, Adelung R, Fiedler B, Schulte K, *Compo Sci and Tech* **60**: 356-365 (2013).

14 Wan Y J, Yang W H, Yu S H, Sun R, Wong C P, Liao W H, *Compo Sci and Tech* **122**:27-35 (2016).

15 Khobragade P S, Hansora D P, Naik J B, Njuguna J, Mishra S, *App Clay Sci* 132–133: 668–674 (2016.)

16 Khobragade P S, Hansora D P, Naik J B, Chatterjee A, *Poly Deg and Stab* **130**:194-244 (2016).

17 Bari P, Lanjewar S, Hansora DP, Mishra S, *Jou of Appl Polym Sci* DOI: 10.1002/app.42927 (2015).

18. Jain R, **Mishra S,** *RSC Adv* 6**:** 27404-27415(2016).

19. Barkade S S, Gajare GR, Mishra S, Naik J B, Gogate P R, Pinjari D V, S H Sonawane, *CRC Press* 868–897(2015).

20. Hansora D P, Shimpi N G, Mishra S, *Journal of Materials* DOI: 10.1007/s11837-015-1522-5 (2015).

21 Song M Y, Cho S Y, Kim N R, Jung S H, Lee J K, Yun Y S, Jin H J, *Carbon* **108**:274-282 (2016).

22 Song J, Gao H, Zhu G, Cao X, Shi X, Wang Y, *Carbon* **95**:1039-1050 (2015).

23 Wu Y, Cao R, Wu G, Huang W, Chen Z, Yang X, Tu Y, *Composites Part A Appl Sci and Manu* **88**:156–164 (2016).

24 Hu Y, Shen J, Li N, Ma H, Shi M, Yan B, Huang W, Wang W, Ye M, *Compo Sci and Tech* **70**:2176–2182 (2010).

25 Hwang S H, Park H W, Park Y B, Um M K, Byun J H, *Compo Sci and Tech* **89**:1-9 (2013).

26 Jin Y, Huang G, Han D, Song P, Tang W, Bao J, Li R, Liu Y, *Composites Part A Appl Sci and Manu* **86**:9-18 (2016).

27 Jin S, Qingzhong X, Qikai G, Yehan T, Wei X, *Composites Part A Appl Sci and Manu* **67**:252–258 (2014).

28 He Z, Zhang B, Zhang H B, Zhi X, Hu Q, Gui C X, Yu Z Z, *Compo Sci and Tech* **102**: 176–182 (2014).

29 Lin Y, Liu S, Peng J, Liu L, *Composites Part A Appl Sci and Manu* **86**:19-30 (2016).

30 Zhang M, Zhang C, Du Z, Li H, Zou W, *Compo Sci and Tech* **138**: 1-7 (2017).

31 Liu K, Chen S, Luo Y, Jia D, Gao H, Hu G, Liu L, *Compo Sci and Tech* **94**:1–7(2014).

32 Hua H, Wang X, Wanga J, Wana L, Liu F, Zheng H, Chen R, Xu C, *Chem Phy Letters* **484**:247–253 (2010).

33 Bortz D R, Heras E G, Gullon I M, *Macromolecules* **45**:238–245 (2012).

34 Chen Y, Zhang H B, Huang Y, Jiang Y, Zheng W G, Yu Z Z, *Compo Sci and Tech* **118**:178-185 (2015).

35 Chatterjee A, Khobragade P, Mishra S, Naik J, *Particuology* **30**:118-128 (2017).

36 Tang Z, Kang H, Shen Z, Guo B, Zhang L, Jia D, *Macromolecules* **45**:3444−3451 (2012).

37 Low F W, Lai C W, Abdhamid S B, *Ceramics International* **41**:5798-5806 (2015).

38 Khobragade P S, Naik J B, Chatterjee A, *Polym Bull* 1-20DOI 10.1007/s00289-016-1812-2 (2016).

39 Khobragade P S, Hansora DP, Naik JB, Njuguna J, *Polym Bull* DOI : 10.1007/s00289-017-1983-5POBU-D-17-00010.1 (2017)

40 Liu C, Yan H, Lv Q, Li S, Niu S, *Carbon* **102**:145-153 (2016).

41 Wang Q, Dai J, Li W, Wei Z, Jiang J, *Compo Sci and Tech* **68**:1644–1648 (2008).

42 Wang H, Xian G, Li H, *Composites Part A Appl Sci and Manu* **76**:172–180 (2015).

43 Baptista R, Mendao A, Guedes M, Mendes R M, *Procedia Structural Integrity* **1**:074–081 (2016).

44 Song Y S, Youn J R, *Carbon* **43**:1378–1385 (2005).

45 Lan T and Pinnavaia T J, *Chem Mater* **6**:2216-2219 (1994).

46 Tong J, Huang H X, Wu M, *Compo Sci and Tech* **129**:183-190 (2016).

47 Shimpi N G, Kakade R U, Sonawane S S, Mali A D, Mishra S, *Polym Plasti Tech and Eng* **50**:758–761 (2011).

48 Tang L C, Wang X, Gong L X, Peng K, Zhao L, Chen Q, Wu L B, Jiang J X, Lai G Q, *Compo Sci and Tech* **91**:63–70 (2014).

49 Wang X, Gong L X, Tang L C, Peng K, Pei Y B, Zhao L, Wu L B , Jiang J X, *Composites Part A Appl Sci and Manu* **69**:288-298 (2015).

50 Ji X, Xu Y, Zhang W, Cui L, Liu J, *Composites Part A Appl Sci and Manu* 2017.

51 Hong N, Zhan J, Wang X, Stec A A, Hull T R, Ge H, Xing W, Song L, Hu Y, *Composites Part A Appl Sci and Manu* **64**:203- 210 (2014).

Captions for Figures

Scheme 1   Possible reaction mechanisms of nPS decorated GO.

Figure 1.   FTIR spectra of (a) Graphite (b) GO (c) nPS (d) nPS decorated GO.

Figure 2   XRD diffraction patterns of (a) Graphite (b) GO (c) nPS (d) nPS decorated GO.

Figure 3.   FE-SEM images of, (a) GO (b) nPS (c) nPS decorated GO.

Figure 4.   TEM images of (a) GO (b) nPS (c) nPS decorated GO.

Figure 5.   Mechanical properties (a) Tensile strength (b) % elongation at break (c) young's
              modulus (d) impact strength.

Figure 6.   TGA curves of (a) GO (b) nPS (c) nPS decorated GO

Figure 7.   TGA curves of (a) epoxy (b) 0.1 (c) 0.2 (d) 0.3 (e) 0.4 (f) 0.5 (g) 0.6 and (h) 0.7 wt.

              % nPS decorated GO filled epoxy nanocomposites.

Figure 8.   Contact angle measurement of (a) epoxy (b) 0.3 (c) 0.5 and (d) 0.7 wt. % nPS decorated

              GO filled epoxy nano composites.

Table 1.   Mechanical and thermal properties of epoxy nano composites.

GO

Styrene
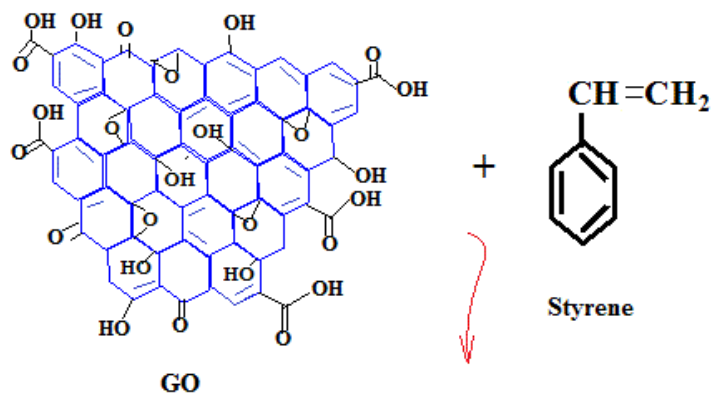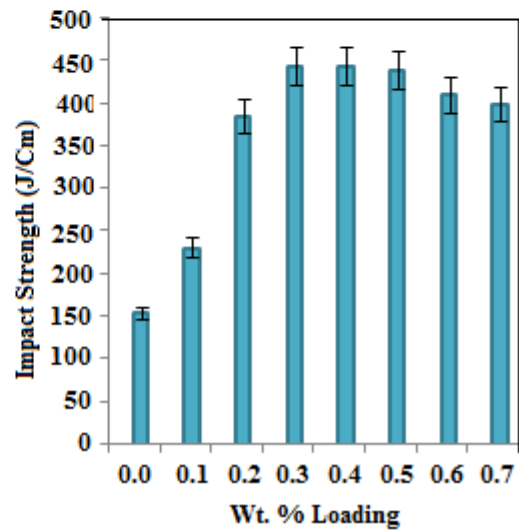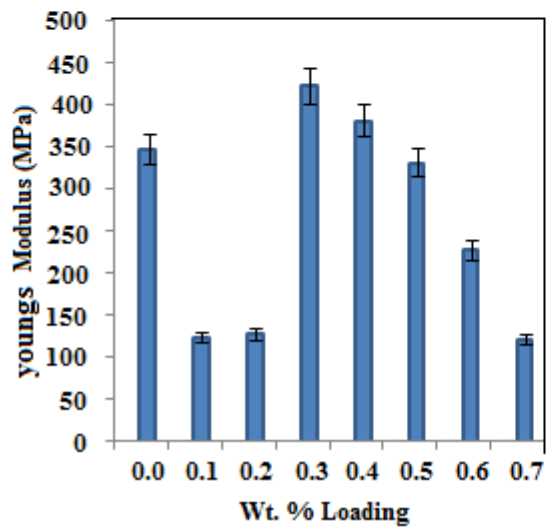
Stepwise Microemulsion
Polymerisation
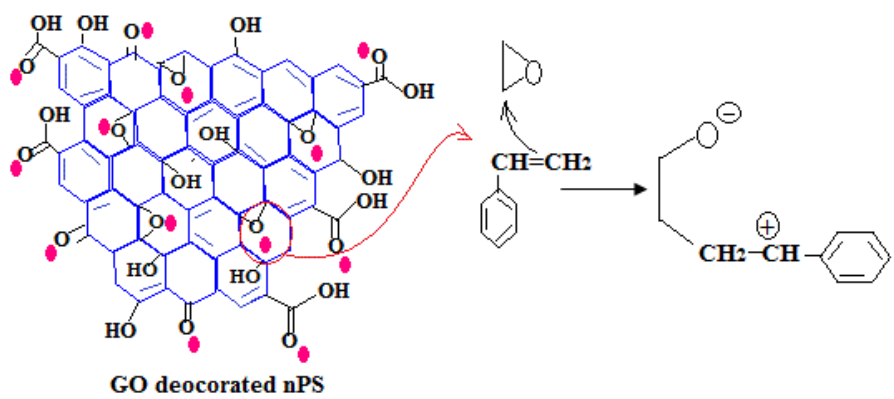
GO deocorated nPS

Scheme 1. Possible reaction mechanisam of nPS decorated GO

(a)   (b)   (c)   (d)

Hydrophillic   Hydrophobic
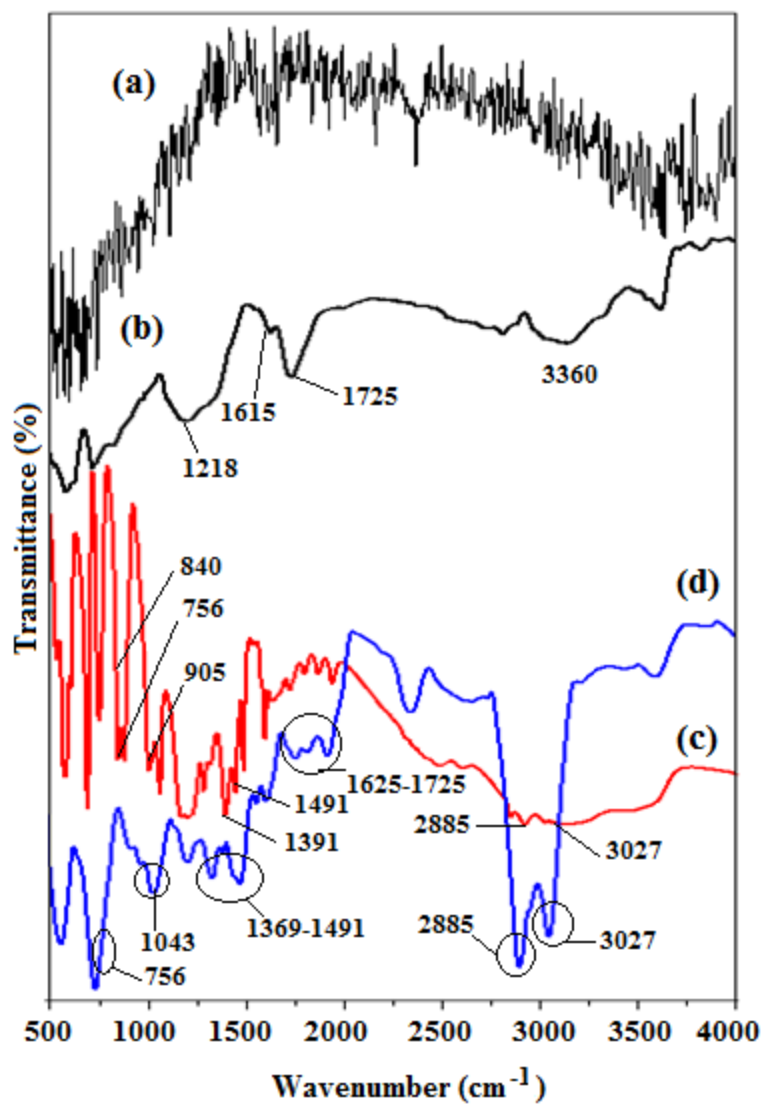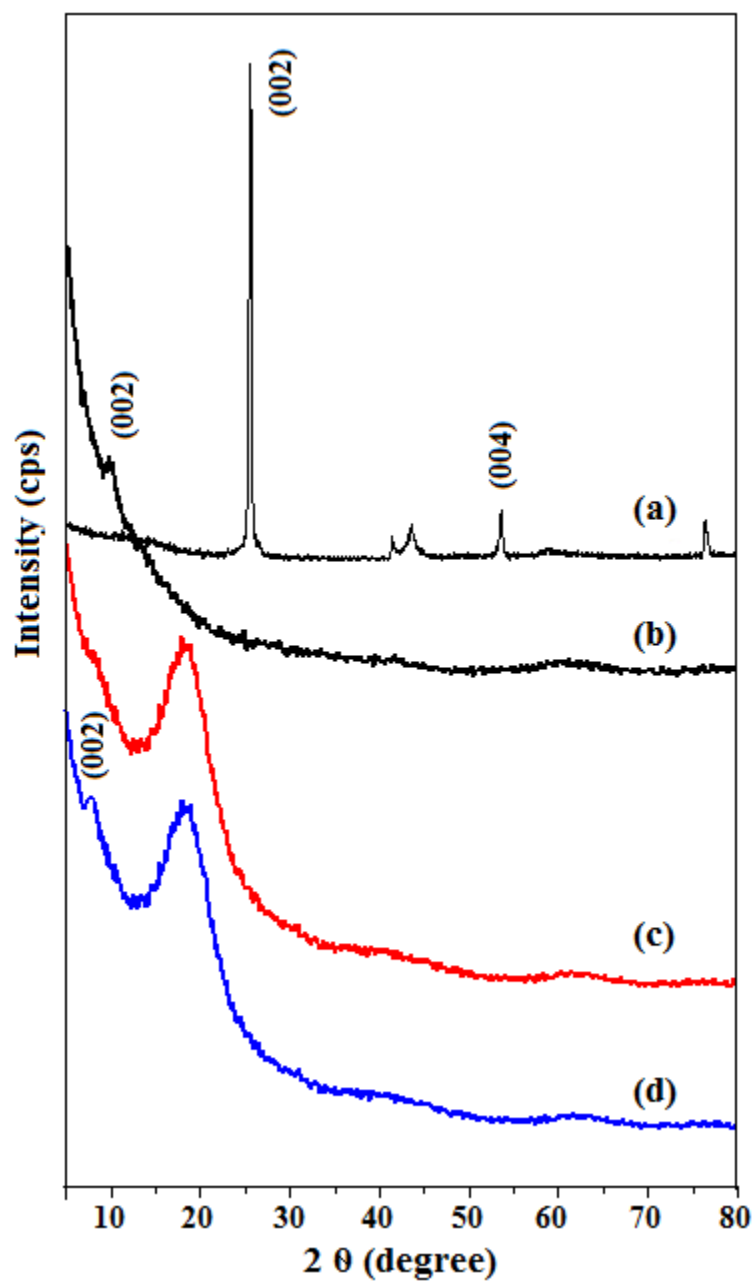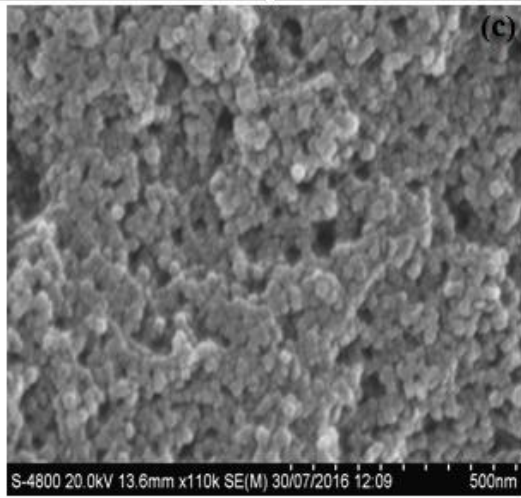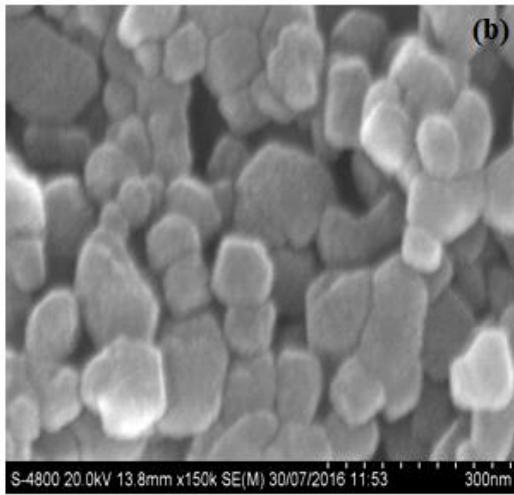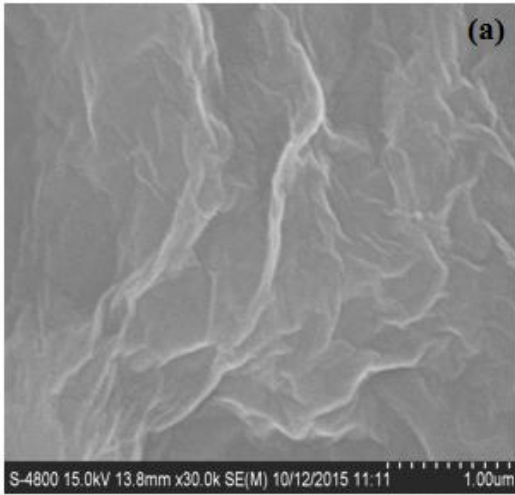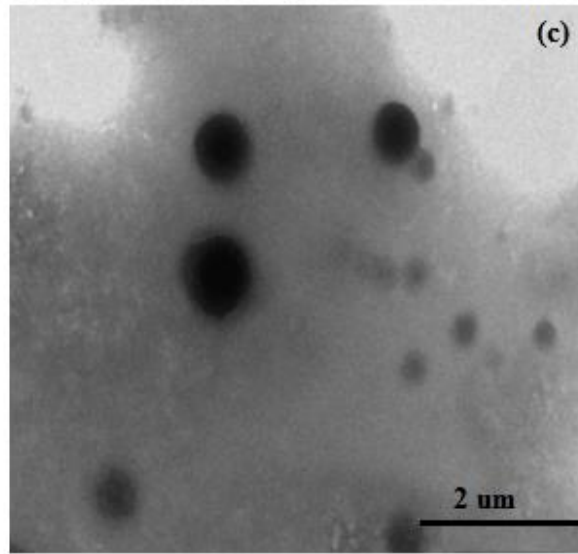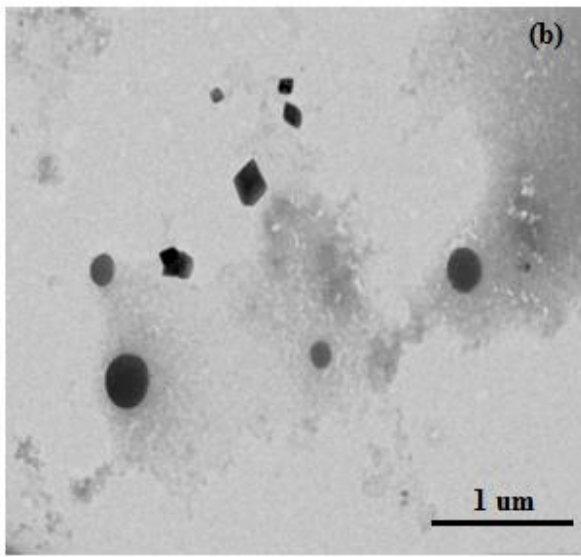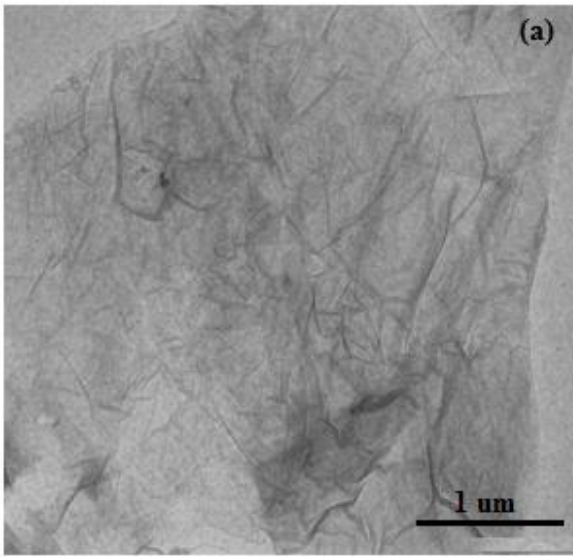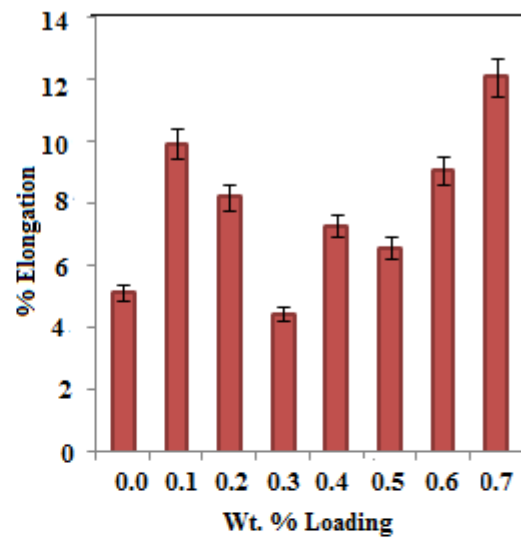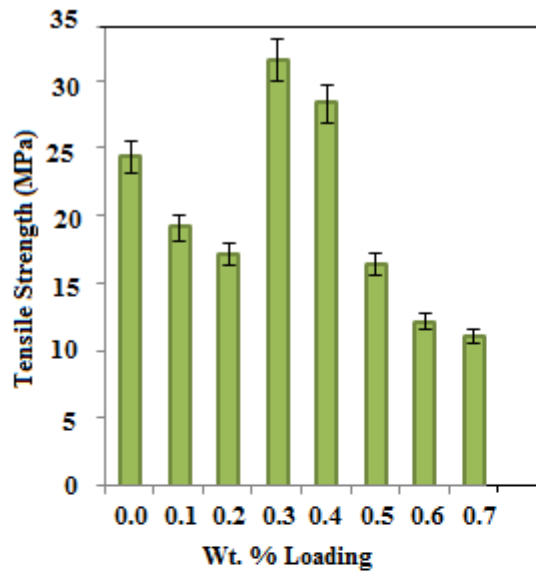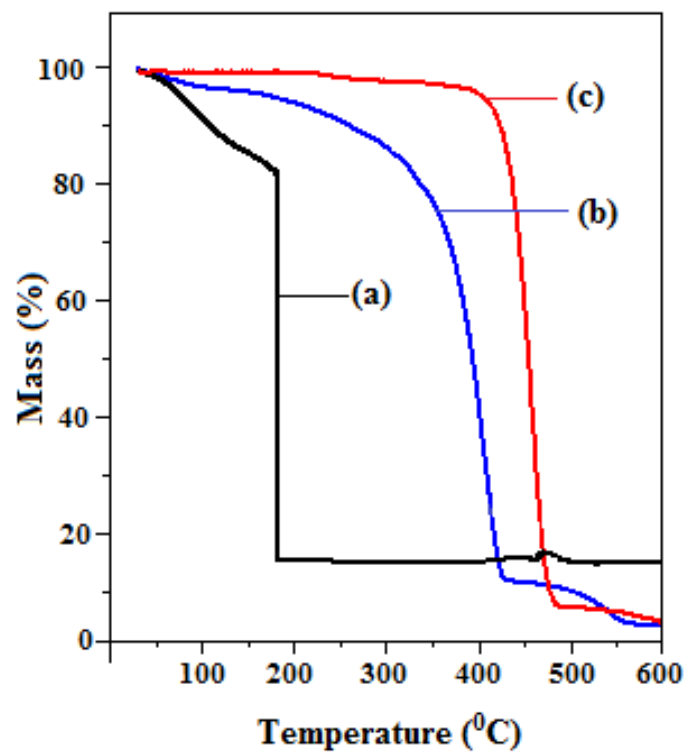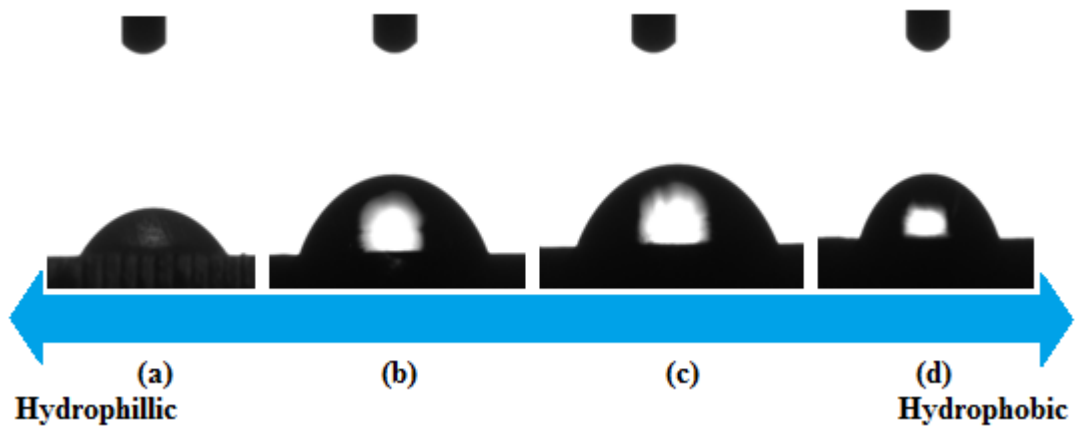
Table 1. Mechanical and thermal properties of epoxy nano composites

Sample composition	Mechanical properties				Thermal properties		
	TS (Mpa)	% Elongation	Young's Modulus (Mpa)	Impact Strength (J/cm)	d_{on} (°C)	d_{off} (°C)	W_L (%)
GO	-	-	-	-	180 ($\pm$1)		90 ($\pm$1)
nPS	-	-	-	-	372 ($\pm$1)		100 ($\pm$1)
nPS-GO	-	-	-	-	424 ($\pm$1)	460 ($\pm$1)	100 ($\pm$1)
Epoxy	24 ($\pm$5)	5 ($\pm$5)	349 ($\pm$5)	154	373 ($\pm$1)	433 ($\pm$1)	85 ($\pm$1)
0.1 wt.%	19 ($\pm$5)	10 ($\pm$5)	124 ($\pm$5)	231	373 ($\pm$1)	439 ($\pm$1)	78 ($\pm$1)
0.2 wt.%	17 ($\pm$5)	8 ($\pm$5)	128 ($\pm$5)	386	374 ($\pm$1)	435 ($\pm$1)	87 ($\pm$1)
0.3 wt.%	32 ($\pm$5)	4 ($\pm$5)	424 ($\pm$5)	444	375 ($\pm$1)	429 ($\pm$1)	85 ($\pm$1)
0.4 wt.%	28 ($\pm$5)	7 ($\pm$5)	382 ($\pm$5)	444	372 ($\pm$1)	424 ($\pm$1)	90 ($\pm$1)
0.5 wt.%	16 ($\pm$5)	7 ($\pm$5)	332 ($\pm$5)	425	376 ($\pm$1)	429 ($\pm$1)	88 ($\pm$1)
0.6 wt.%	12 ($\pm$5)	9 ($\pm$5)	228 ($\pm$5)	410	379 ($\pm$1)	434 ($\pm$1)	89 ($\pm$1)
0.7 wt.%	11 ($\pm$5)	12 ($\pm$5)	122 ($\pm$5)	746	366 ($\pm$1)	423 ($\pm$1)	95 ($\pm$1)